Yuzhou Chen
Department of Reactor Engineering Research and Design,
China Institute of Atomic Energy,
P.O. Box 275(59),
Beijing 102413, China
e-mail: chenyz2015@icloud.com

Minfu Zhao
Department of Reactor Engineering Research and Design,
China Institute of Atomic Energy,
P.O. Box 275(59),
Beijing 102413, China
e-mail: zhaominfu@163.com

Keming Bi
Department of Reactor Engineering Research and Design,
China Institute of Atomic Energy,
P.O. Box 275(59),
Beijing 102413, China
e-mail: bikeming@126.com

Bin Yang
Department of Reactor Engineering Research and Design,
China Institute of Atomic Energy,
P.O. Box 275(59),
Beijing 102413, China
e-mail: 270513461@qq.com

Dongxu Zhang
Department of Reactor Engineering Research and Design,
China Institute of Atomic Energy,
P.O. Box 275(59),
Beijing 102413, China
e-mail: Dongxu2007@yeah.net

Kaiwen Du
Department of Reactor Engineering Research and Design,
China Institute of Atomic Energy,
P.O. Box 275(59),
Beijing 102413, China
e-mail: ciae_dukaiwen@163.com

Critical Heat Flux of Flowing Water in Tube for Pressure Up to Near Critical Point—Experiment and Prediction

Critical heat flux (CHF) experiment with uniform heating was performed in a tube of 8.2 mm in inner diameter and 2.4 m in heated length. The water flowed upward through the test section. The pressure covered the range from 8.6 to 20.8 MPa, mass flux 1157 to 3776 kg/m^{2}s, inlet quality −2.79 to −0.08 (subcooling 19–337 °C), and local quality −0.97 to 0.53. For the pressure close to the near-critical point, the CHF decreased substantially with the pressure increasing. For the subcooling larger than a certain value, the CHF was related to the local condition. But for low subcooling and saturated condition, the CHF was related to the total power. The present results were in agreement with the previous experiment for the same local subcooled condition. Based on the present experimental results with subcooled and saturated conditions an empirical relation of the CHF was presented. [DOI: 10.1115/1.4038215]

Keywords: critical heat flux, near-critical pressure, subcooled and saturated condition

1 Introduction

The critical heat flux (CHF) is a major concern to the design of nuclear reactors, because it is an important limitation for their operation. Great number of investigations has been available in the literature, including the experimental and theoretical researches. Up to now, various empirical correlations, theoretical predictions, and the look-up tables for the CHF have been proposed for the design of the reactors [1–13]. A comprehensive review of the researches has been presented [14]. In recent years, the supercritical water-cooled reactors are selected as the candidate of Gen-IV reactors due to its high efficiency and more safety. But only limited experiments of the critical heat flux were performed for the near-critical pressure, and some parametric trends were studied [15–17].

In the author's previous study, the experiments of subcooled flowing water were performed in the uniform heating tubes of inner diameters from 2.32 to 16 mm for pressure of 0.1–2 MPa and from 4.62 to 10.89 mm for pressure of 2–20.6 MPa [18]. The empirical correlations and theoretical predicted method were proposed. In this study, the experiment was extended to the saturated condition with heating tube of 8.2 mm in inner diameter and 2.4 m in heated length. The mass flux was extended to a high value, and an empirical correlation was proposed.

2 Experimental Facility and Procedure

The experimental facility is shown in Fig. 1. The deionized water is driven by a canned pump. Then, it flows through the

Manuscript received May 1, 2017; final manuscript received October 16, 2017; published online December 4, 2017. Assoc. Editor: Thomas Schulenberg.

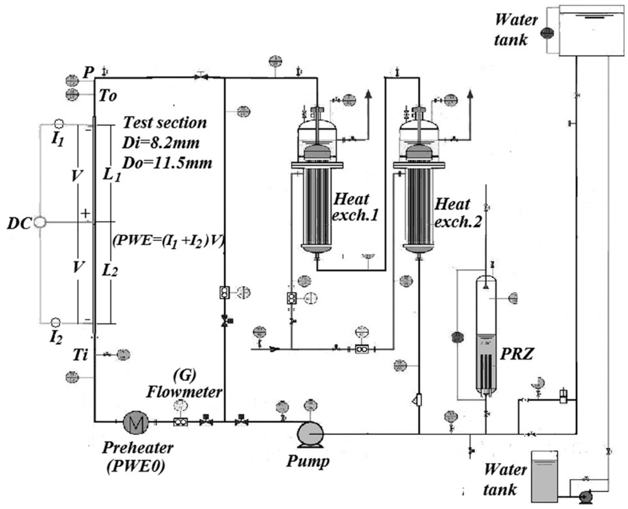

Fig. 1 The diagram of test loop

flowmeter, the preheater, and upward through the test section. Finally, it passes to the heat exchangers and then back to the pump. The pressure is kept by the pressurizer. The test section is an Inconel-600 tube of 8.2 mm in inner diameter, 11.5 mm in outer diameter, and 2.4 m in heated length.

The K-type sheathed thermocouples of 1 mm in diameter are used to measure the inlet and outlet water temperatures of the test section. The turbine flowmeters of 6 and 10 mm in diameter are used to measure the flow rate. The outlet pressure is measured by a pressure transducer. The AC supply with capacity of 160 kW is used for the preheating. The DC supply with capacity of 7000 A $\times$ 65 V is applied for the test section by two subsections in parallel, as shown in the figure. The voltage and the currents to the each subsection are measured. The onset of CHF is detected by the photocells. At normal operation condition, the photocell does not have any output. While when the wall temperature increases to above 500 °C, the photocell produces an electrical signal. The onset of CHF is always detected at near the end of test section. This simple method has been used for the CHF experiments with uniform heating for more than 40 years without any failure, especially for a larger tube where the location of the onset of CHF is difficult to expect accurately [19]. The reliability of the occurrence of CHF is validated by the reproduction of the CHF data in many tests. All the experimental data are recorded by a

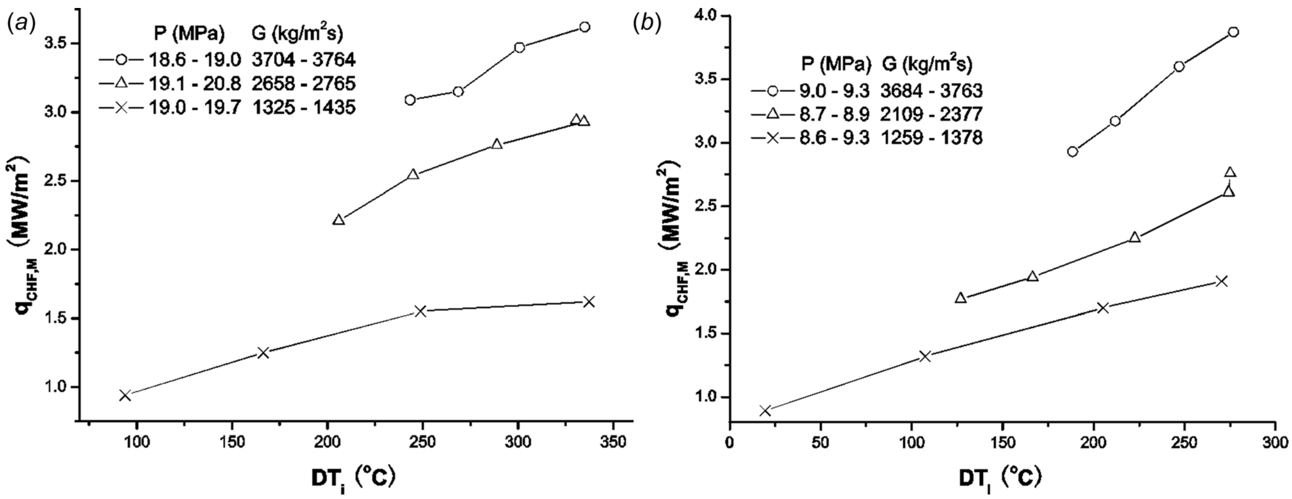

Fig. 2 The variations of CHF with the inlet subcooling for different mass fluxes: (*a*) P = 18.6–20.8 MPa and (*b*) P = 8.6–9.3 MPa

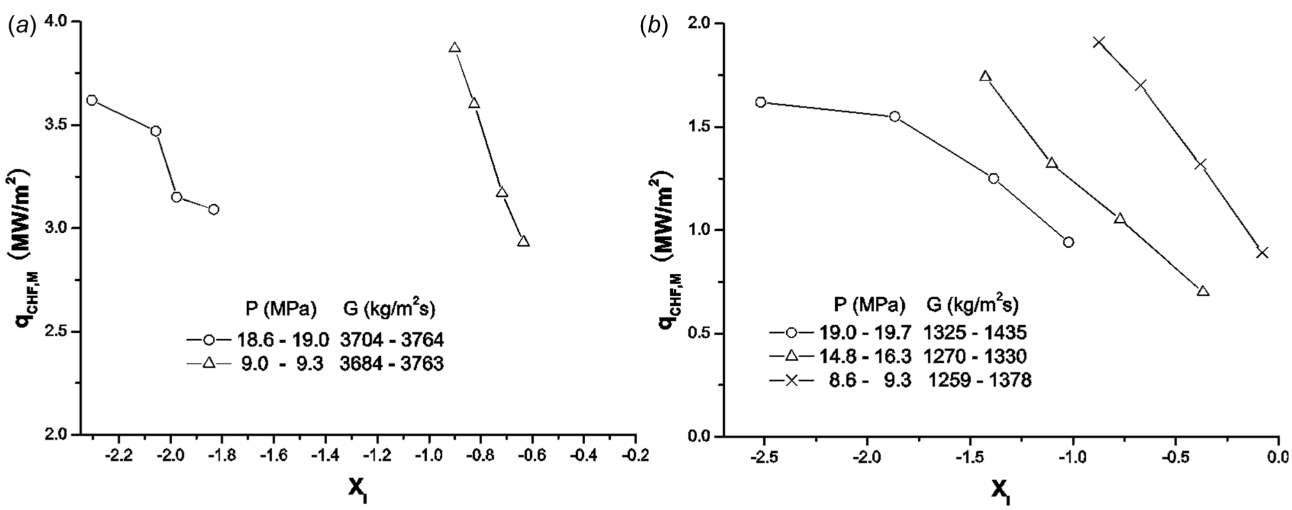

Fig. 3 The variations of CHF with the inlet quality for different pressures: (*a*) G = 3684–3764 kg/m^{2}s and (*b*) G= 1259–1435 kg/m^{2}s

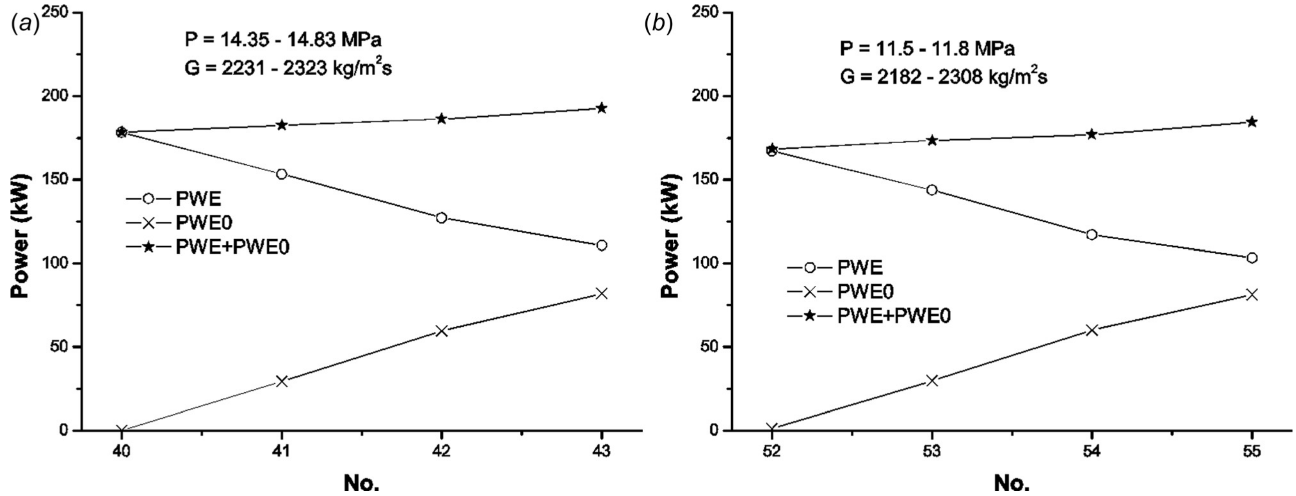

Fig. 4 The variations of powers to the test section and the preheater: (*a*) $P = 14.35$–14.83 MPa, $G = 2231$–2323 kg/m^{2}s and (*b*) $P = 11.5$–11.8 MPa, $G = 2182$–2308 kg/m^{2}s

Table 1 The geometries and experimental conditions in the previous experiment

D/L (mm/m)	P (MPa)	G (kg/m^{2}s)	DT_i (°C)	DT_o (°C)	$q_{CHF,M}$ (MW/m^2)	Data
4.62/0.5	1.8–20.6	556–4055	110–354	1–169	0.77–9.3	118
7.98/0.8	2.0–20.4	476–1653	53–361	3–158	0.26–4.95	193
10.89/1.1	1.7–20.0	454–1144	169–345	4–141	0.92–3.3	74

data acquisition system. The uncertainty for the water temperatures is ±2.0 °C, the flow rate ±1.0%, the pressure ±0.5%, the current and voltage ±0.5%, and the critical heat flux ±1.5%.

During experiment, the pressure was controlled by the pressurizer, and the flow rate was controlled by valves at a required value. A certain preheating power was applied to keep the inlet water temperature, and the heating power to the test section was increased gradually. When the CHF condition was closed, the power to the test section was increased very slowly. Until the onset of CHF condition was detected, the power was shut down. Then, another run was started at a required pressure, flow rate, and inlet water temperature with slow increase of the power to the test section. For the near-critical pressure, at the onset of critical condition, the increase of surface temperature appears not so sharp as lower pressure.

3 Experimental Results

Totally, 72 CHF data points were obtained, covering the ranges of pressure of 8.6–20.8 MPa, mass flux of 1157–3776 kg/m^{2}s, inlet subcooling of 19–337 °C and local subcooling of 0–92.7 °C or local quality of −0.97 to 0.53. The power to the test section was nearly axial uniform. The critical heat flux was evaluated at the up subsection by $V \times I_1$/3.1416/D/L, where D was the inner diameter, V was the voltage, I_1 and L_1 were the current and the length of up heated section. For subcooled outlet condition, the local (outlet) subcooling was from the measurement. While for saturated condition, the local quality was determined from the inlet subcooling with heat balance equation.

3.1 The Effects of Parameters on the CHF. The effect of inlet subcooling on the CHF with different mass fluxes is shown in Fig. 2, and the effect of inlet quality on the CHF with different pressures is shown in Fig. 3. For all the conditions, the CHF is increased as the mass flux increasing. It is also increased as the inlet subcooling increasing or decreased as the inlet quality increasing. When the pressure closes to the near-critical point, the trend of CHF with inlet subcooling is not so strong as lower pressure. This effect is more evident in the figures of $q_{CHF,M} - X_i$, as seen in Fig. 3, because at higher pressure the latent heat of evaporation decreases remarkably.

3.2 The Variation of Total Power With a Given Mass Flux for a Saturated Condition. For the saturated condition, keeping the pressure and mass flux nearly constant, the inlet temperatures ahead of the preheater remained in a small range (22–31 °C). When the power to the preheater, PWE$_0$, was increased from 0 to about 90 kW, the powers to the test section, PWE, varied correspondingly. The PWE, PWE$_0$, and the sum of PWE and PWE$_0$ were shown in Fig. 4. It was interesting to see that at saturated condition, with different PWE$_0$, the sum of PWE and PWE$_0$ varied very small. This appears to be in agreement with the finding that for the quality larger than a certain value the critical quality is determinant [20].

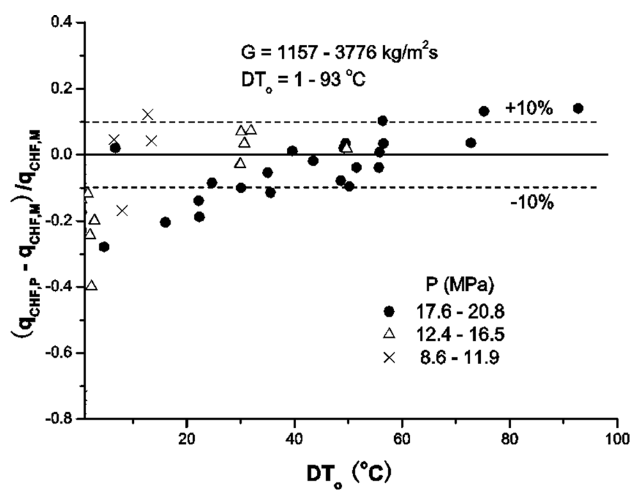

Fig. 5 The comparison of the present experimental results of subcooled conditions with the previous empirical correlations

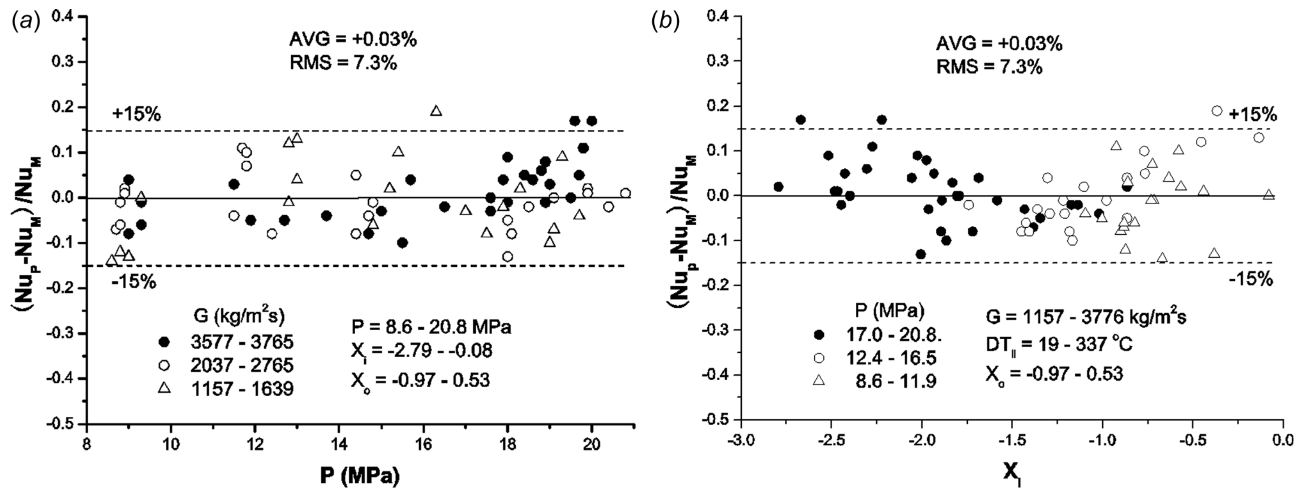

Fig. 6 The comparison of the present experimental results with the empirical correlation

4 Comparison of the Present Results With the Previous Correlation

In the previous study, an empirical correlation was proposed to formulate the subcooled experimental results of $D = 4.62$, 7.98, and 10.89 mm with heated lengths of 0.5, 0.8, and 1.1 m, respectively [18]. The conditions are listed in Table 1. The empirical correlation is as follows:

$$q_{\mathrm{CHF}} = c q_s \tag{1}$$

where

$$q_s = \frac{(H_s - H_i)GD}{4L} \tag{2}$$

and

$$c = \min\left[\frac{2350(1 - 0.0307P)}{\left(G(H_s - H_i)D/0.008\right)^{0.35}}, 1.0\right] \tag{3}$$

where the H_s and H_i are the liquid saturated enthalpy and the inlet enthalpy in J/kg, the P is the pressure in MPa, G is the mass flux in kg/m^{2}s, D and L are the diameter and heated length in m. In these tests, the ratio L/D is nearly 100. Therefore, to compare the present results of subcooled condition with this correlation, the H_i is calculated at the location $L = 0.82$ m from the end of heating by heat balance, H_{100}, and Eq. (2) is written as $q_s = (H_s - H_{100})G/400$. Then, the comparison is made by $(q_{\mathrm{CHF},P} - q_{\mathrm{CHF},M})/q_{\mathrm{CHF},M}$ versus DT_o, where the $q_{\mathrm{CHF},P}$, and $q_{\mathrm{CHF},M}$, are the predicted and measured CHF, respectively. As shown in Fig. 5, for the local subcooling larger than 25 °C, the agreements are nearly within ±10%, which is the same as the original experiment. However, at lower subcooling, the deviation appears increased. It is concluded that for higher subcooled condition, the CHF is related to the local condition, but for low subcooled and low quality condition, the total power is related [20].

5 The Present Empirical Correlation

Totally, 72 experimental data are obtained, covering the ranges of $P = 8.6$–20.8 MPa, $G = 1157$–3776 kg/m^{2}s, $DT_{\mathrm{i}} = 19$–337 °C, and $X_0 = -0.97$ to 0.53. The experimental results are formulated by the following empirical correlation

$$q_{\mathrm{CHF}} = c q_0 \tag{4}$$

where

$$q_0 = \frac{(1 - X_0)GDH_{fg}}{4L} \tag{5}$$

and

$$c = 1 - 0.00216(GH_{fg})^{0.25} \tag{6}$$

where q_{CHF} and q_0 are the critical heat flux and heat flux in W/m^2, G is the mass flux in kg/m^{2}s, H_{fg} is the latent heat of evaporation in J/kg, the D and L are the diameter and heated length in m.

The comparison of the experimental data with the present correlation is shown in Fig. 6. For more than 95% data points, the deviations are less than 15%, and the average error and the root-mean-square error are +0.03% and 7.3%, respectively.

6 Conclusions

The critical heat flux experiment of flowing water was performed under subcooled and saturated conditions in the uniform heated tube of 8.2 mm in diameter and 2.4 m in heated length, covering the ranges of pressure of 8.6–20.8 MPa, mass flux of 1157–3776 kg/m^{2}s, inlet subcooling of 19–337 °C, and local quality of −0.97 to 0.53. The following conclusions were achieved:

(1) The CHF is increased as the inlet subcooling or mass flux increasing. For higher local subcooling condition, the CHF is related to the local parameters, but for low subcooling or saturated condition, the CHF is related to the total power. At higher quality condition, the critical quality is determinant.
(2) For the pressure near-critical point, the trend of $q_{\mathrm{CHF}} - X_i$ is not so strong as lower pressure, and at the onset of CHF, the surface temperature is increased not so remarkably.
(3) For higher local subcooling, the experimental results agree with the previous correlation. For the present subcooled and saturated condition, an empirical correlation is presented.

Acknowledgment

The present investigation is supported by the International Atomic Energy Agency Coordinated Research Program (IAEA Renewal contract 18341/R3).

Nomenclature

AVG = average error $(1/n)\sum_{i=1}^{n}((q_{\mathrm{CHF},P} - q_{\mathrm{CHF},M})/q_{\mathrm{CHF},M})$
c = correction factor
D = Inner diameter, m
DT_i = inlet subcooling, °C

DT_o = local (outlet) subcooling, °C
G = mass flux, kg/m^{2}s
H_{fg} = latent heat of evaporation, J/kg
H_i = inlet enthalpy, J/kg
H_s = saturated liquid enthalpy, J/kg
H_{100} = enthalpy at the location of 0.82 m from the heated end, J/kg
L = heated length, m
L_1 = heated length at up subsection, m
L_2 = heated length at low subsection, m
No = run number
P = pressure, MPa
PWE = power to the test section, kW
PWE$_0$ = power to the preheater, kW
q_{CHF} = critical heat flux, W/m^2
$q_{\mathrm{CHF},M}$ = measured critical heat flux, W/m^2
$q_{\mathrm{CHF},P}$ = predicted critical heat flux, W/m^2
q_s = heat flux for $X_o = 0.0$, W/m^2
q_0 = heat flux for $X_o = 1.0$, W/m^2
RMS = root-mean-square-error $\left((1/n)\sum_{i=1}^{n}\left((q_{\mathrm{CHF},P} - q_{\mathrm{CHF},M})/q_{\mathrm{CHF},M}\right)^2\right)^{0.5}$
X_i = inlet quality
X_o = local (outlet) quality

References

[1] Berglest, A. E., 1977, "Burnout in Boiling Heat Transfer—Part II: Subcooled and Low Quality Forced-Convection System," Nucl. Saf., **18**(2), pp. 154–167.
[2] Komori, Y., Kaminaga, M., Sakurai, F., Ando, H., Sudo, Y., Saito, M., and Futamura, Y., 1991, "Safety Criterion for Burnout of the Plate-Type Fuel in Pressurized Conditions," Third Asian Symposium on Research Reactor, Hitachi, Japan, Nov. 11–14, pp. 190–197.
[3] Knoebel, D. H., Harris, S. D., Crain, B., Jr., and Biderman, R. M., 1973, "Forced Convection Subcooled Critical Heat Flux," Savannah River National Laboratory, Aiken, SC, Technical Report No. DP-1306.
[4] Zeiganik, Y. A., 1994, "Critical Heat Flux and Pressure Drop Under Forced Convection Boiling of Subcooled Water: Experimental Data," Tenth International Heat Transfer Conference (IHTC), Brighton, UK, Aug. 14–18, pp. 581–586.
[5] Kirillov, P. L., and Yushenko, S. S., 1996, "Diameter Effect on CHF," Second Research Coordination Meeting, IAEA Coordinated Research Program on Thermal-hydraulics Relationships for Advanced Water Cooled Reactors, Vienna, Austria.
[6] Weisman, J., and Pei, B. S., 1983, "Prediction of Critical Heat Flux in Flow Boiling at Low Qualities," Int. J. Heat Mass Transfer, **26**(10), pp. 1463–1477.
[7] Sudo, Y., and Kaminaga, M., 1993, "A New CHF Correlation Scheme Proposed for Vertical Rectangular Channels Heated From Both Sides in Nuclear Research Reactors," Trans. ASME, **115**(2), pp. 426–434.
[8] Celata, G. P., Cuma, M., Mariani, A., Simosini, M., and Zummo, G., 1994, "Rationalization of Existing Mechanistic Models for the Prediction of Water Subcooled Flow Boiling Critical Heat Flux," Int. J. Heat Mass Transfer, **37**(Suppl. 1), pp. 347–360.
[9] Katto, Y., 1992, "A Prediction Model of Subcooled Water Flow Boiling CHF for Pressures in the Region 0.1–20.0 MPa," Int. J. Heat Mass Transfer, **35**(5), pp. 1115–1123.
[10] Lee, C. H., and Mudawar, I., 1988, "A Mechanistic Critical Heat Flux Model for Subcooled Flow Boiling Based on Local Bulk Flow Conditions," Int. J. Multiphase Flow, **14**(6), pp. 711–728.
[11] Doroshchuk, V. E., Levitan, L., and Lantzman, F. P., 1975, "Investigation Into Burnout in Uniformly Heated Tubes," ASME Paper No. 75-WA/HT-22.
[12] Groeneveld, D. C., Leung, L. K. H., Kirillov, P. L., Bobkov, V. P., Smogalev, I. P., Vinogradov, V. N., Huang, X. C., and Royer, E., 1996, "The 1995 Look-Up Table for Critical Heat Flux in Tubes," Nucl. Eng. Des., **163**(1–2), pp. 1–23.
[13] Pernica, R., and Cizek, J., 1995, "General Correlation for Prediction of Critical Heat Flux Ratio for Water Cooled Channels," Seventh International Meetings of Nuclear Reactor Thermal-Hydraulics (NURETH), Saratoga, NY, Sept. 10–15, Paper No. NUREG/CP-0142.
[14] IAEA, 2001, "Thermohydraulic Relationships for Advanced Water Cooled Reactors," International Atomic Energy Agency, Vienna, Austria, Report No. IAEA-TECDOC-1203.
[15] Vijayarangan, B. R., Jayanti, S., and Balakrishan, A. R., 2006, "Studies on Critical Heat Flux in Flow Boiling at Near Critical Pressures," Int. J. Heat Mass Transfer, **49**(1–2), pp. 259–268.
[16] Chun, S. Y., Hong, S. D., Kikura, H., and Aritomi, M., 2007, "Critical Heat Flux in a Heater Rod Bundle Cooled by R-134a Fluid Near the Critical Pressure," Nucl. Sci. Technol., **44**(9), pp. 1189–1198.
[17] Yin, S. T., Lui, T. J., Huang, Y. D., and Tain, R. M., 1988, "Measurements of Critical Heat Flux in Forced Flow at Pressures Up to the Vicinity of the Critical Point of Water," National Heat Transfer Conference, Houston, TX, July 24–27, pp. 501–506.
[18] Chen, Y., Bi, K., Zhao, M., Yang, C., and Du, K., 2016, "Critical Heat Flux With Subcooled Flowing Water in Tubes for Pressures From Atmosphere to Near-Critical Point," J. Energy Power Eng., **10**(4), pp. 211–222.
[19] Chen, Y., and Sheng, W., 1979, "Detection of the Onset of Critical Heat Flux by Photocell," The Predictions and Experiments in Nuclear Reactors—Nuclear Reactor Thermal-Hydraulics, Press of Atomic Energy (in Chinese), p. 00054452.
[20] Tong, L. S., and Tang, Y. S., 1997, *Boiling Heat Transfer and Two-Phase Flow*, 2nd ed., Taylor & Francis, Abingdon, UK.